

Colorimetric Effect of Au Nanoparticle Chain/Polymer Film under Mechanical Stress and Gas Pressure

Gowoon Shim¹, Kiryung Eom¹, Gyuyeon Lee¹ and Hyungtak Seo^{1,2†}

¹Department of Energy Systems Research, Ajou University, Suwon 16499, Republic of Korea

²Materials Science and Engineering, Ajou University, Suwon 16499, Republic of Korea

(Received October 10, 2017 : Revised October 10, 2017 : Accepted November 3, 2017)

Abstract Gas detection is necessary for various reasons, including the prevention of gas leakages and the creation of necessary environmental conditions. Among the gas detection methods, leakage of gas can be confirmed using materials that undergo color changes that are easily distinguished by the naked eye. Metal nanoparticles (NPs) experience variations in their absorption wavelengths under the localized surface plasmon effect (LSPR) with mechanical stresses, which change the distance between NPs. In this study, we attempted to detect the presence of gas utilizing the LSPR-related color change of a chain of Au NPs. The assembly of Au NPs, arranged in a chain shape, experienced a color change from dark blue to purple with a change in the distance between the NPs by applying a physical force, *i.e.*, compression, stretching, and gas pressure. As the force of compression and the degree of stretching increased, the absorption wavelength shifted from doublet peaks at 650 and 550 nm to a singlet peak at 550 nm. Further, applying gas pressure caused an identical color change. With this result, we propose a method that could be applied to all gases that require detection based on gas pressure.

Key words Au nanoparticles, assembly, colorimetric, mechanical stress, gas pressure.

1. Introduction

The need for gas sensors is increasing due to safety and environmental issues. The method of detecting the gas by the color change is very suitable as the safety sensor because it is easy to distinguish the gas leakage by the naked eye. Usually, it is a chemical sensor, which is equipped with a specific gas sensor depending on the gas to be detected.¹⁻²⁾ However, there is also a need for a concept of a gas sensor applicable to all gases that are not limited to specific gases or low-reactivity gases.

Metal nanoparticles (NPs) show colors when illuminated by light because they display plasmon resonance. That is, colloidal NPs of plasmonic noble metals, which exhibit localized surface plasmon resonance (LSPR), have scattering and absorption ranges in the visible spectrum.³⁻⁴⁾ Plasmonic NPs show tunable optical properties because of their sizes and shapes; the structure of a NP assembly and the number of NPs in the assembly also induce tuning of plasmon excitations.⁵⁻⁷⁾

Assemblies of Au NPs have recently been applied in

general and biological sensing applications because of their optical and electronic properties, in addition to the electronic coupling between adjacent particles that can generate many new properties, such as hot spots. These can cause increased efficiency in surface-enhanced Raman scattering (SERS).⁸⁻⁹⁾

The optical properties of plasmonic NPs can be controlled by adjusting the distances separating the Au NPs in an assembly by applying chemical or mechanical forces.¹⁰⁻¹²⁾ Another study developed a linear assembly of Au NPs that could be reversibly disassembled by modifying the Au NPs with sufficiently strong ligands; they also demonstrated a chain film of Au NPs (Au film) that showed a colorimetric response to mechanical forces.¹³⁻¹⁴⁾

In this work, the change of optical properties in an assembly of plasmonic NPs, specifically a chain of Au NPs, is induced by mechanical stresses. The Au NP chain was prepared according to another study.¹⁴⁾ Here, we demonstrated the disassembly of the chain by stretching, compressing, and applying the pressure of gases, which can also drive the breakage of the Au NP chain

[†]Corresponding author

E-Mail : hseo@ajou.ac.kr (H. Seo, Ajou Univ.)

© Materials Research Society of Korea, All rights reserved.

This is an Open-Access article distributed under the terms of the Creative Commons Attribution Non-Commercial License (<http://creativecommons.org/licenses/by-nc/3.0>) which permits unrestricted non-commercial use, distribution, and reproduction in any medium, provided the original work is properly cited.

and cause a color change in the Au film. This functionality was used to visually confirm the leakage of gases by observing the change in the film color caused by the elevated pressure of leaking gas. This is a new way to check for the presence of gases and is not specific to a particular gas, unlike most conventional chemical methods.

2. Experimental procedure

2.1 Synthesis of Au NPs

The 15-nm spherical Au NPs were synthesized using a previously reported process.¹⁴⁾ In a reactor fitted with a reflux condenser, 95 mL of 0.02 wt% aqueous HAuCl_4 was heated to 80–90 °C with magnetic stirring, followed by the injection of 5 mL 1 wt% aqueous trisodium citrate. After 30 min of reaction, the color of the solution changed from yellow to ruby red. The product was cooled to room temperature of 30 °C or less, mixed with 20 mg of bis(p-sulfonatophenyl) phenylphosphine (BSPP), and stirred at 100 rpm for 24 h. After ligand exchange, the BSPP-capped Au NPs were centrifuged at 12,000 rpm for 30 min and washed thrice, followed by re-dispersion in de-ionized (DI) water and final dispersion in 1 mL DI water.

2.2 Assembly of Au NP chains

Aqueous solutions of NaCl (15 μL , 0.1 M) and ethanol (4.485 mL) were sequentially added to 0.5 mL of the Au NP stock solution. After gentle shaking, the solution was allowed to stand for 1 h to form Au NP chains, during which its color changed from ruby to deep blue.

2.3 Fabrication of Au films

Polyvinylpyrrolidone (PVP, 0.1 g, M.W. = 360,000) and polyethylene glycol (PEG, 4 %) were added to the 1-mL Au NP chain suspension. The mixture (0.6 mL) was used to fill a polydimethylsiloxane (PDMS) mold (1.5 \times 1.5 cm), which was placed in a vacuum oven for 3–4 h at 40 °C. Solid films were peeled off from the mold. These had a thickness of 250 μm for the stretching and gas pressurization tests; circular-shape films were cut with diameters of 13 mm using a puncher for compression testing.

2.4 Compression test

Samples were loaded into a pressing die and a constant force was applied to the die for 1 min using a hand-press.

2.5 Stretching test

Samples were fixed to clamps on either side and stretched to a certain length at constant speed and held for 1 min.

2.6 Gas pressurization

In the gas pressurization test, gas was applied at a pressure of 100 psi at a distance of 5 cm from the film. Air was blown using an air compressor (Seowon, Korea), and 100 % N_2 gas was used in the gas cylinder. The pressure of the gas was read from the gas gauge.

2.7 Characterization

Optical absorption profiles of the films were measured using an ultraviolet-visible light (UV-vis) spectrophotometer (Avantes, Netherlands). High-resolution transmission electron microscopy (HRTEM) images were obtained using a Tecnai G2 F30 S-Twin microscope (Japan) of the Au NP solution samples deposited on a Cu grid at an accelerating voltage of 200 kV.

3. Results and Discussion

A schematic of Au film preparation is shown in Fig. 1.¹⁴⁾ After the ligands of the citrate-capped Au NPs were replaced with BSPP, a stronger ligand than citrate, the BSPP-capped Au NPs were assembled into linear chains by adding ethanol and NaCl to weaken the electrostatic repulsion between the NPs. At this stage, the color of the solution changed from ruby to deep blue. PVP was then dissolved in the solution to forming a matrix for the Au chains, blocking the aggregation of the Au NPs and ensuring uniform dispersion. The final Au chain solution was then prepared by adding 6 wt% PEG to allow the smooth motion of Au NPs under applied stress. The PDMS mold was filled with the solution and the dried Au-chain film, having a thickness of 250 μm , was then

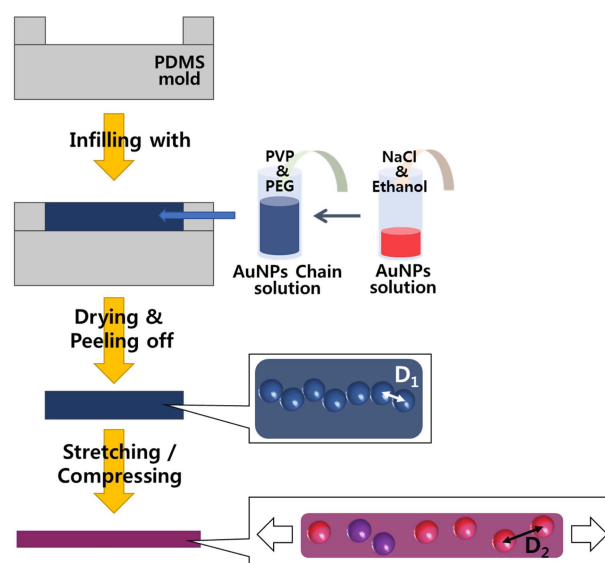


Fig. 1. The schematic of preparation of Au NPs chain/polymer film (D: Interparticle distance, $D_1 < D_2$).

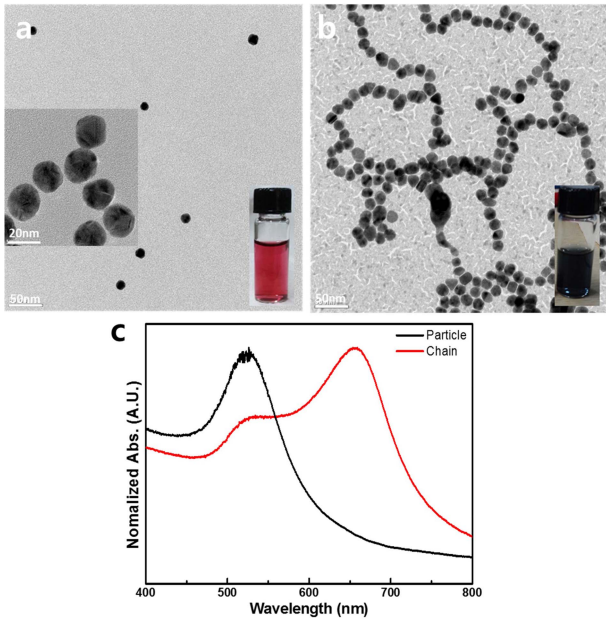


Fig. 2. (a), (b) TEM images and (c) absorption spectra of Au NPs and Au chain solutions.

peeled off. The original color of the film was deep blue, similar to that of the Au NP chain solution. The color changes of the film were recorded with applied compression and tension relative to this initial state.

A uniform dispersion of Au particles with the average size of 15 nm is observed by HRTEM (Fig. 2(a, b)). When the ethanol and NaCl solutions are added, it is seen that the Au NPs are connected to form linear Au NP chains. TEM images of single Au NPs and the chain Au NPs are also shown. The solution of single Au particles is ruby-colored, while the Au chain solution is dark blue. The optical absorption spectra of the two solutions differ: the single-Au-particle solution has a single peak at 550 nm, while the Au chain solution exhibits a low-intensity peak at 550 nm and a high-intensity peak at 650 nm (Fig. 2(c)).

In this experiment, an Au film with a diameter of 13 mm was compressed. The film was initially dark blue, the same as the color of the Au chain solution, and showed a strong absorption peak at 650 nm and a broad and low peak at 550 nm. The sample was placed on a hand-press. Strong forces of 9280 and 13,900 psi were applied for 1 min each, and the absorption changes of the film are as shown in Fig. 3. Under the applied force of 9280 psi, the high-intensity peak at 650 nm shifts to approximately 620 nm and overlaps with the broad peak at 550 nm. This means that the chains of Au NPs are slightly broken. Under the higher applied force of 13,900 psi, the double absorption peaks merge into a single absorption peak at 550 nm. Stronger compressive forces applied to Au film correspond to greater blue shifts in

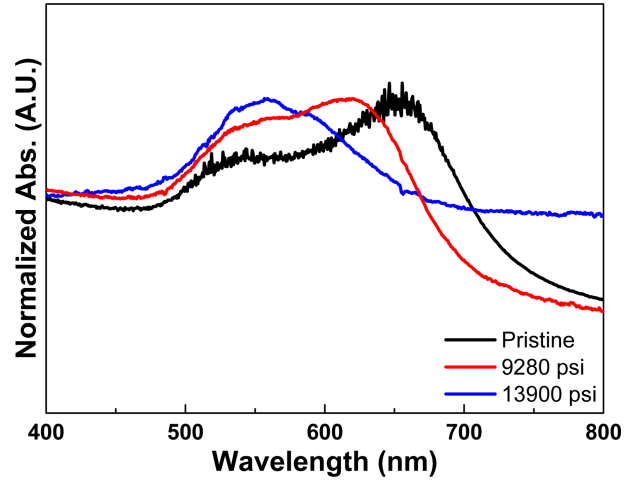


Fig. 3. Absorption spectra of Au film after compression at different pressures.

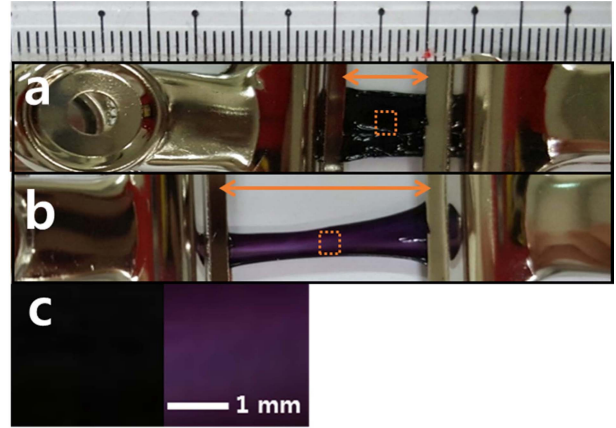


Fig. 4. Photographs of Au film. (a) Pristine, (b) stretched, and (c) color changes of Au film under different stretching forces.

the absorption peaks, as more of the chains are broken and the interparticle distance increases.

Fig. 4 shows the method for the stretching test of the film. Both ends of the film are held by the clamps and the film is stretched from 1 (Fig. 4(a)) to 2 cm (Fig. 4(b)) in length. It is observed that the dark blue film turns purple; Fig. 4(c) reveals each color in enlarged regions of the film with and without stretching. The color changes because, as in the compression test, the Au NPs are separated from each other; accordingly, the absorption wavelengths of the Au plasmon particles are changed.

Fig. 5(a) shows the change of the absorption spectra according to the stretching of the film from 1 to 7 cm by 1-cm increments. The changes in absorption when the film is stretched are similar to those of the compression experiment described above. The film at 1 cm initially has two absorption peaks, a high-intensity peak at

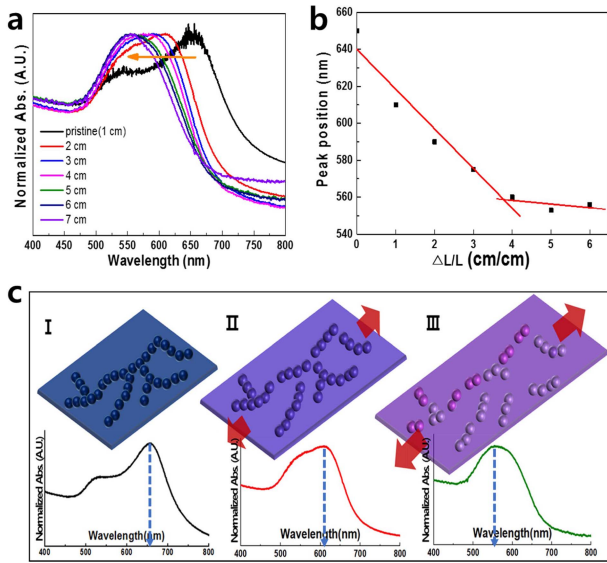


Fig. 5. (a) Absorption spectra of Au film after stretching to different lengths, (b) change in peak position as a function of $\Delta L/L$, and (c) schematic of stretching test for Au film.

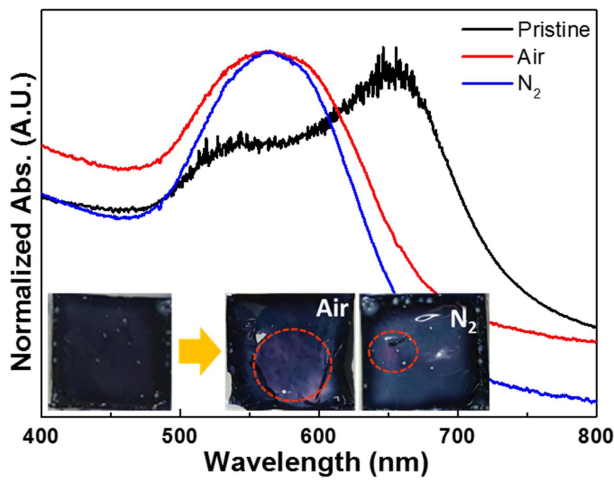


Fig. 6. Absorption spectra of Au film during the injections of air and N₂ gas (Insets: Photographs of Au film).

650 nm and a relatively low-intensity peak at 550 nm. Under stretching to 2 cm, the high peak shifts to 610 nm. The two peaks then approach each other because of the separation of the Au NP chains. Consequently, as the length of film is increased by 1-cm increments, the distances between Au NPs in the chains are increased, so that the absorption spectra of the film reveal the merging of the doublet peaks into a singlet peak at 550 nm. This is because the Au NP plasmonic absorption wavelength changes depending on the assembly size of the Au NP chain. The results suggest that longer stretching lengths correspond to greater degrees of chain breakage in our study.⁶⁾ The chain breakage is physically equivalent to

the decreasing assembly size of the Au NPs, causing the shift of the plasmonic peak to shorter wavelengths. Based on the above, the peak positions were plotted as a function of elongation, $\Delta L/L$ (Fig. 5(b)). The peak position linearly decreases as a function of elongation for up to 4 cm. On the other hand, for $\Delta L/L$ exceeding 5 cm, the position of the peak remains nearly constant. This is because the long Au chains are broken and the peaks of the absorptions are shifted to a single short wavelength, and therefore overlap each other. That is, the long Au chain is cut apart and the absorption peaks are shifted to short wavelengths overlapping to form a single peak. After that, the less-broken short chain is broken further, and the full width at half maximum (FWHM) of the absorption peak is slightly reduced (Fig. 5(c) I \rightarrow II \rightarrow III).

In the above, the Au film was subjected to uniaxial compressive and tensile forces, and the color changes of the film under these forces were confirmed. Both forces are included when gas is applied to the film. Therefore, we consider that gas pressure can be a driving force to change the color of the film. Gas at a pressure of 100 psi was applied at a distance of 5 cm from the film. At the gas applied area, the dark blue turned purple and the absorption spectrum is shown (Fig. 6 and insets). Regardless of the type of the gas, both N₂ and air cause the area to change color and the absorption peak is shifted from 650 nm to 550 nm (Fig. 6). When the N₂ gas is applied, the area where the gas is applied to the film is widened so that the force is weakened and the FWHM is larger than when the air is applied. Thus, this experiment demonstrates the possibility of detecting gas leakages by gas-pressure-sensitive color-changing films. In many industrial circumstances, the instantaneous and precise detection of gas leakage is required, regardless of the gas type, for safety purposes to allow rapid initial actions to be taken. However, conventional gas sensors working by chemoelectrical methods have sensing ranges limited to specific gas types, slow sensing kinetics, and various errors in function because of noise gas effects and others. This gas leakage-sensing platform, based on the pressure-sensitive plasmonic effect, offers the alternative principle of naked-eye-detectable gas sensing.

4. Conclusion

In this study, Au nanoparticles were fabricated into a chain structure that was then made into a film. The changes in the spectral absorption of the film, according to applied compression and tension, were observed. The initial dark blue film with an absorption spectrum peak at 650 nm showed a peak shift toward the shorter wavelength of 550 nm visibly changed to purple in color under increasing compressive forces and tensile elongation

lengths. In this way, the absorption wavelength of the NPs was changed by the gas pressure, and the color of the film also changed observably when either air or N₂ gas was applied. The method of detecting a gas by causing a color change under an applied pressure is applicable to any gas species for detection, rather than being limited to a specific gas. This new method differs significantly from the conventional chemical gas sensor detection method. It could be applied by further optimizing the substrate film and developing protective layers for machinery.

Acknowledgement

This research was supported by the Basic Science Program through the National Research Foundation(NRF) (NRF-2015R1A2A2A01003790), which is funded by the Ministry of Science, ICT, and Future Planning of the Republic of Korea.

References

1. Y.-A. Lee, S. S. Kalanur, G. Shim, J. Park and H. Seo, *Sens. Actuators B*, **238**, 111 (2017).
2. S. S. Kalanur, I.-H. Yoo, Y.-A. Lee and H. Seo, *Sens. Actuators B*, **221**, 411 (2015).
3. K. Schröder and A. Csáki, *SPIE Newsroom*, 15 June 2011 from <http://spie.org/newsroom/3692-plasmonic-tuning-of-optical-fibers-for-biosensing>
4. S. A. Maier, *Plasmonics: Fundamentals and Applications*, Springer Science & Business Media LLC, 233 Spring Street, New York, NY 10013, USA (2007).
5. J. Yguerabide and E. E. Yguerabide, *Anal. Biochem.*, **262**, 137 (1998).
6. Z. Zhong, S. Patskovskyy, P. Bouvrette, J. H. T. Luong and A. Gedanken, *J. Phys. Chem. B*, **108**, 4046 (2004).
7. A. Gabudean, D. Biro and S. Astilean, *Nanotechnology*, **23**, 485706 (2012).
8. S. A. Meyer, E. C. Le Ru and P. G. Etchegoin, *Anal. Chem.*, **83**, 2337 (2011).
9. Y. Zhang, W. Chu, A. D. Foroushani, H. Wang, D. Li, J. Liu, C. J. Barrow, X. Wang and W. Yang, *Materials*, **7**, 5169 (2014).
10. U. Cataldi, R. Caputo, Y. Kurylyak, G. Klein, M. Chekini, C. Umeton and T. Bürgi, *J. Mater. Chem. C*, **2**, 7927 (2014).
11. A. Rankin and S. McGarry, *Nanotechnology*, **26**, 075502 (2015).
12. H. Zhang and D. Wang, *Angewandte Chemie Int. ed.*, **120**, 4048 (2008).
13. X. Han, J. Goebel, Z. Lu and Y. Yin, *Langmuir*, **27**, 5282 (2011).
14. X. Han, Y. Liu and Y. Yin, *Nano lett.*, **14**, 2466 (2014).